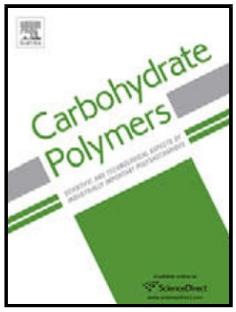

Title: Vancomycin-loaded chitosan aerogel particles for chronic wound applications

Authors: Clara López-Iglesias, Joana Barros, Inés Ardao, Fernando J. Monteiro, Carmen Alvarez-Lorenzo, José L. Gómez-Amoza, Carlos A. García-González

PII: S0144-8617(18)31188-3
DOI: https://doi.org/10.1016/j.carbpol.2018.10.012
Reference: CARP 14144

To appear in:

Received date: 13-3-2018
Revised date: 14-9-2018
Accepted date: 5-10-2018

Please cite this article as: López-Iglesias C, Barros J, Ardao I, Monteiro FJ, Alvarez-Lorenzo C, Gómez-Amoza JL, García-González CA, Vancomycin-loaded chitosan aerogel particles for chronic wound applications, *Carbohydrate Polymers* (2018), https://doi.org/10.1016/j.carbpol.2018.10.012

Vancomycin-loaded chitosan aerogel particles for chronic wound applications

Clara López-Iglesias[a], Joana Barros[b], Inés Ardao[c], Fernando J. Monteiro[b], Carmen Alvarez-Lorenzo[a], José L. Gómez-Amoza[a], Carlos A. García-González[a,*]

[a]*Departamento de Farmacología, Farmacia y Tecnología Farmacéutica, R+D Pharma group (GI-1645), Facultad de Farmacia and Health Research Institute of Santiago de Compostela (IDIS), Universidade de Santiago de Compostela, E-15782 Santiago de Compostela, Spain*

[b]*FEUP-Faculdade de Engenharia, Universidade do Porto, I3S-Instituto de Investigação e Inovação em Saúde, and INEB-Instituto de Engenharia Biomédica, 4200-135 Porto, Portugal*

[c]*BioFarma Research group, Centro Singular de Investigación en Medicina Molecular y Enfermedades Crónicas (CiMUS), Universidade de Santiago de Compostela, E-15782, Santiago de Compostela, Spain*

Corresponding author: carlos.garcia@usc.es; *phone: +34 881 815252; fax: +34 981 547148*

Keywords: chitosan; aerogel; chronic wounds; antimicrobial

GRAPHICAL ABSTRACT

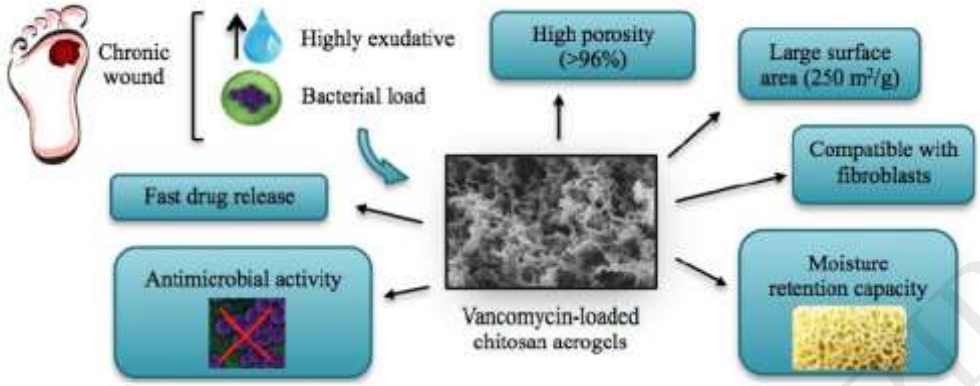

Highlights

- Vancomycin-loaded chitosan aerogels were prepared for chronic wound management
- Chitosan aerogels exhibited low-density, large surface area and high porosity
- Aerogels can provide a fast local administration of vancomycin at the wound site

Abstract

Chronic wounds are a prevailing cause of decreased quality of life, being microbial burden a factor hindering the normal wound healing process. Aerogels are nanostructured materials with large surface area (>250 m^2/g) and high porosity (>96%). In this work, vancomycin-loaded chitosan aerogel beads were tested as a potential formulation to treat and prevent infections at the wound site. Processing of chitosan in the form of aerogels endowed this polysaccharide with enhanced water sorption capacity and air permeability. The morphological and textural properties of the particles were studied by image and N_2 adsorption-desorption analysis and scanning electron microscopy. Vancomycin content and release profiles from aerogel carriers showed a fast drug release that permitted to efficiently achieve local therapeutic levels. Cell studies with fibroblasts and antimicrobial tests against *S. aureus* showed that the particles vancomycin-loaded aerogels were cytocompatible and effective in preventing high bacterial loads at the wound site.

1. Introduction

The healing process under normal physiological conditions in response to an injury comprises a series of steps (hemostasis, inflammation, proliferation and resolution) that lead to the complete replacement of the damaged tissue (Harper, Young, & McNaught, 2014; Li, Chen, & Kirsner, 2007). However, the healing process is hampered in chronic wounds such as diabetic foot ulcers, venous leg ulcers and pressure ulcers and remains in the inflammatory phase for prolonged periods of time (Morton & Phillips, 2016). Prospective studies indicate that the incidence of chronic wounds will increase because of poor health habits and the progressive ageing of the population (Gosain & DiPietro, 2004).

Hypoxia, changes in pH and microbial burden are among the factors hindering the normal healing process resulting in a chronic wound (Guo & DiPietro, 2010). Thus, materials for wound management should possess good oxygen permeability to avoid hypoxia and permit a normal cell metabolism. They should also have a high aqueous fluid recruitment to favor a correct exudate management (Bajjada, 2017). On the other hand, the use of materials for the local treatment and prevention of infections in the wound site is an auspicious solution for the treatment of chronic wounds (Hiriart-Ramírez et al., 2012; Luna-Straffon et al., 2014).

Products in the form of gauzes, foams, hydrocolloids and other types of dressings are already commercially available for the treatment of chronic wounds (Dhivya, Padma, & Santhini, 2015). The world market for wound management is increasing with expected sales of $21.85 billion by year 2021 (Driscoll, 2016). Particularly, it can be forecasted that the market share of new technologies and materials for wound management, e.g., endowed with antimicrobial properties, will have outstanding growth prospects with respect to traditional dressings.

Aerogels are nanostructured dry materials with high porosity (>95%) and large surface area (>300 m^2/g) that can provide advanced performances for wound healing (García-González, Alnaief, & Smirnova, 2011; Govindarajan et al., 2017; Pierre & Pajonk, 2002). This particular porous structure of aerogels allows fast initial water ingress and can also act as a carrier for bioactive compounds with high loading capacity, enhanced stability upon storage and accelerated drug release (Maleki et al., 2016). Aerogels are usually obtained from the drying of

organic, inorganic or hybrid gels with supercritical CO_2 ($scCO_2$), which avoids the pore collapse in the gel network typical of other drying methods and represents a green, safe and innovative technology (Şahin, Özbakır, İnönü, Ulker, & Erkey, 2018). The technology is versatile in terms of composition, but aerogels to be applied in biological systems must be made of biocompatible, non-toxic and preferably biodegradable materials (Maleki et al., 2016). Polysaccharides represent a suitable choice for the preparation of aerogels for wound applications (García-González et al., 2011; García-González & Smirnova, 2013). In this regard, chitosan is of particular interest since it can gather together antimicrobial activity against Gram(+) and Gram(-) bacteria, hemostatic activity and stimulation capability of tissue regeneration at the wound site (Jayakumar, Prabaharan, Sudheesh Kumar, Nair, & Tamura, 2011; Muzzarelli, 2011). Chitosan forms part of some conventional wound dressings approved by regulatory agencies (e.g. Tegasorb®, HemCon®, ChorioChit®) (Ahmed & Ikram, 2016; Kumar, Muzzarelli, Muzzarelli, Sashiwa, & Domb, 2004; Niekraszewicz, 2005; Rinki, Dutta, Hunt, Macquarrie, & Clark, 2011; Wu, Zivanovic, Draughon, Conway, & Sams, 2005) but, to the best of our knowledge, there are no chitosan-based products in the market using chitosan in the form of aerogels.

Chitosan is obtained by deacetylation of chitin in a degree of 50% or higher and its physicochemical properties are characterized by its deacetylation degree and molecular weight. These properties will influence the chitosan solubility in aqueous solutions and their antimicrobial activity (Chang, Lin, Wu, & Tsai, 2015; Younes, Sellimi, Rinaudo, Jellouli, & Nasri, 2014). Chitosan dissolves in dilute acids through the protonation of its free amino groups, allowing its processing into different gel formulations by sol-gel methods. When the chitosan solution is put in contact with a basic medium, the amino groups of the polysaccharide deprotonate and the polymer precipitates forming the three-dimensional fibrous network of the gel. Chitosan aerogels can then be obtained by supercritical drying of the gels (Kayser et al., 2012; Quignard, Valentin, & Di Renzo, 2008; Rinki et al., 2011).

Chitosan aerogels are of special interest as drug carriers for wound applications that demand a prompt therapeutic level of bioactive agent is needed at high exuding environment and shortly

after debridement. In contrast to other chitosan-based materials (nanoparticles, xerogels, cryogels, sponges) loaded with drugs, chitosan aerogels encompass the properties of aerogels for exudate management and carrier for bioactive agents, along with the properties of chitosan in terms of biological performance and ability of the chemical structure to interact with active molecules (Ahsan et al., 2017; Buzia, Dima, & Dima, 2015; Cerchiara et al., 2017; S.-H. Chang et al., 2015; Pawar, Boateng, Ayensu, & Tetteh, 2014). As bioactive agent to be loaded in the aerogel, vancomycin is a glycopeptide antibiotic widely used parenterally for the treatment of infected wounds in hospitalized patients due to its broad range of efficacy against Gram-positive bacteria, and is specially indicated under suspicion of infection by methicillin-resistant *S. aureus* (Kosinski & Lipsky, 2010). Vancomycin may also have a limited antimicrobial effect against Gram-negative bacterial strains (García-González et al., 2018; Liu, Lee, Wang, & Liu, 2015). The direct local application of vancomycin powder alone instead of intravenous infusion was proposed for surgical wounds with low accessibility during the clinical procedure (e.g., in spine surgery) with relative success, although the risk of microbial wound recolonization and delayed infections was highlighted due to the reduction of the vancomycin concentration over a postadministration timeframe of 1 to 3 days (Zebala et al., 2014). The local administration of vancomycin is thus an alternative therapy and the incorporation of vancomycin in a formulation able to provide a local and controlled delivery of the drug into the wound site is an auspicious solution to reduce the administered dose as well as the risk of appearance of bacterial drug resistance (Bakhsheshian, Dahdaleh, Lam, Savage, & Smith, 2015; Noel, Courtney, Bumgardner, & Haggard, 2010; O'Neal & Itani, 2016; Xiong, Pan, Jin, Xu, & Hirche, 2014). In case of accessible wound sites, the relevance of a local treatment with vancomycin using dressings with specific release characteristics and retained moisture for wound healing has been reinforced with clinical studies proving the bacterial load reduction in the wound (Albaugh, Biely, & Cavorsi, 2013). For this case, the change of these dressings is preferred every 1-3 days, the usual exchange frequency used for wound management in nursery (NHS NEW Devon CCG, 2018).

In this work, chitosan aerogels loaded with bioactive agents are herein evaluated for the first time regarding their capacity to treat and prevent infections in chronic wounds. Vancomycin-loaded chitosan aerogel beads were prepared by the sol-gel method followed by gel drying with $scCO_2$. The obtained aerogels were analyzed in terms of morphological, textural and physicochemical properties. The vancomycin content in the chitosan aerogels and its release profile in phosphate buffer solution (PBS pH 7.4) at 37 ºC were evaluated. The antimicrobial activity against a *Staphylococcus aureus* bacterial strain, the collagenase activity, the cytocompatibility with fibroblasts and the water sorption capability of the chitosan aerogels were specifically tested to reduce the microbial burden at the wound site after debridement.

2. Materials and methods

2.1. Materials

Chitosan (deacetylation degree 90%, viscosity 1000 mPa·s, M_w 200-400 kDa) was supplied by Heppe Medical Chitosan GmbH (Halle, Germany). Vancomycin hydrochloride (M_w 1486 g/mol, 94.3% purity, amorphous) was supplied by Guinama (Valencia, Spain). Collagenase from *Clostridium histolyticum* (Type I, 0.26 FALGPA units/mg solid), N-(3-[2-furyl]acryloyl)-Leu-Gly-Pro-Ala (FALGPA), Fetal Bovine Serum (FBS) and penicillin 10,000 U/mL – streptomycin 10 mg/mL were supplied by Sigma-Aldrich (Saint Louis, MO, USA). BALB/3T3 clone A31 mouse fibroblasts (ATCC CCL-163) and Dulbecco's modified Eagle's medium (DMEM) were from the American Type Culture Collection (ATCC, Manassas, VA, USA). Glacial acetic acid and absolute ethanol (EtOH) were both purchased from VWR (Radnor, PA, USA). NaOH (98.0% purity) and HCl (35%, w/w) were from Panreac (Barcelona, Spain) and Labkem (Barcelona, Spain), respectively. CO_2 (99.8% purity) was supplied by Praxair (Madrid, Spain). Water was purified using reverse osmosis (resistivity >18 MΩ·cm, MilliQ, Millipore®, Madrid, Spain).

2.2. Preparation of chitosan aerogel beads

2.2.1. Preparation of the chitosan hydrogel

Hydrogel particles were prepared following the sol-gel method. Firstly, chitosan powder was dissolved in Milli-Q water containing 1% (v/v) of acetic acid to a final concentration of 2.5 %

(w/v). The solution was mechanically stirred for 10 min and then left to settle for 3 h to eliminate gas bubbles formed during the agitation. Thereafter, 8 mL of the chitosan solution were transferred to a plastic syringe (nozzle diameter of 2 mm) and added dropwise to 50 mL of a gelation bath of NaOH 0.1 M at a constant flow rate of 0.65 mL/min using a syringe pump (AL-1000, World Precision Instruments, Sarasota, FL, USA). Droplets gelified just after contact with the NaOH solution and hydrogel beads were formed. These beads were left in the gelation bath for different ageing times (0.5, 1, 2, 4, 10 and 24 h). In the case of vancomycin-loaded aerogels, vancomycin hydrochloride powder was added to the chitosan solution (i.e. the *sol*) in a content of 5, 10 and 20 % (w/w of chitosan). Aerogels were denoted as CS*x*-V*y*, where *x* is the ageing time (h) and *y* is the theoretical content of vancomycin (% w/w of chitosan).

2.2.2. Solvent exchange

The gelation bath was poured out of the beaker containing the gel beads and immediately replaced by 50 mL of absolute EtOH to get *ca.* 60-70 alcogel particles. After 30 min, a second solvent exchange with a similar volume of EtOH was carried out to eliminate any remnant of water in the gel particles.

2.2.3. Supercritical extraction of the gel solvent

Alcogel particles were introduced into paper cartridges and put into the 100-mL autoclave of the supercritical equipment (Thar Process, Pittsburg, PA, USA). 20 mL of EtOH were previously added to the said pressurized vessel to avoid the premature evaporation of the EtOH contained in the alcogels before reaching the supercritical conditions of the CO_2-EtOH mixture (García-González, Camino-Rey, Alnaief, Zetzl, & Smirnova, 2012). During the 3.5 h-duration drying process, a scCO_2 flow of 5 g/min passed through the autoclave where the gels were contained at a processing temperature and pressure of 40 ºC and 120 bar, respectively. The extracted liquid ethanol was sampled at selected drying times to monitor the kinetics of the supercritical process (Fig. S-1).

2.3. Characterization

2.3.1. Physicochemical properties of the gel beads

Images of hydrogel, alcogel and aerogel chitosan particles were taken with a digital camera and analyzed with ImageJ v1.49 software (U.S. National Institutes of Health, Bethesda, MD, USA) to measure the diameter and volume of the beads and thus to calculate the volume shrinkage during each processing step. Values were obtained from the analysis of *ca.* 25 particles.

The envelope density (ρ_{env}) of the aerogel beads was calculated as the ratio between the average particle weight obtained with a precision balance (80A-200M, Precisa, Dietikon, Switzerland) and the dimensions obtained by image analysis. Chitosan aerogel beads were compared to xerogels and cryogels obtained from the same alcogel precursors by oven drying (37 ºC) and freeze-drying (-85 ºC, vacuum), respectively. Skeletal density (ρ_{skel}) was measured by helium pycnometry (MPY-2, Quantachrome, Delray Beach, FL, USA) at 25 ºC and 1.03 bar from six replicates. The overall porosity (ε) of the dried gels was expressed in percentage and calculated according to Eq. (1):

$$\varepsilon = \left(1 - \frac{\rho_{env}}{\rho_{skel}}\right) \times 100 \qquad (1)$$

The textural properties of the aerogel particles were characterized by nitrogen adsorption-desorption analysis (ASAP 2000, Micromeritics, Norcross, GA, USA). The Brunauer-Emmet-Teller (BET) and the Barrett-Joyner-Halenda (BJH) methods were applied to calculate the specific surface area (a_{BET}) and the pore size distribution, respectively (Sing, 2009). The overall specific pore volume ($V_{p,BJH}$) and the mean pore diameter ($D_{p,BJH}$) were also obtained from the BJH method. The specific mesopore volume (V_{mes}) was obtained from the cumulative BJH-pore volume profiles of the aerogels in the mesopore range (2-50 nm). The specific volume occupied by the macropores (V_{MP}) in the aerogels was calculated as the difference between the total specific pore volumes of the aerogels (i.e. the inverse of the envelope density) and the specific pore volume occupied by mesopores (V_{mes}). The surface structure of the aerogel beads was also studied by Scanning Electron Microscopy at 3 kV with a secondary electron detector (SEM, EVO LS15, Zeiss, Oberkochen, Germany). Aerogels were previously sputtered-coated (Q150T S/E/ES, Quorum Technologies, Lewes, UK) with a thin layer (10 nm) of iridium to improve the contrast.

Crystallinity of the raw materials and the aerogels was studied by X-ray diffraction (XRD, PW-1710, Philips, Eindhoven, The Netherlands) in the 2-50º 2Θ-range using a 0.02º step and Cu $K\alpha_1$ radiation.

Attenuated total reflectance/Fourier-Transform Infrared Spectroscopy (ATR/FT-IR) was performed using a Gladi-ATR accessory equipped with a diamond crystal (Pike, Madison, WI, USA). Solid samples of pure chitosan, pure vancomycin and unloaded and vancomycin-loaded chitosan aerogel beads were characterized in the mid-IR spectrum range (400 – 4000 cm^{-1}) using 32 scans at a resolution of 2 cm^{-1}.

2.3.2. Water absorption assay

The swelling behavior of chitosan aerogel particles obtained at different ageing times was tested in 50 mL of PBS solutions of pH 6.0, 7.0 and 8.0 under magnetic stirring (250 rpm) and in triplicate. Ten chitosan aerogel beads of known weight (*ca.* 15 mg) were used for each experiment. Particles were introduced into stainless steel baskets to put the whole aerogel surface in contact with the fluid, thus preventing particles from floating. At specific soaking times (0.5, 1, 2, 4, 8 and 24 h), particles were collected and weighed after having their surface water slightly wiped with filter paper. Water uptake at each time was calculated using Eq. (2):

$$\text{Water absorption (\%)} = \frac{w_t - w_0}{w_0} \times 100 \qquad (2)$$

where w_t is the weight of the wet particles at time t, and w_0 is the initial weight of the dry particles.

2.3.3. Collagenase activity test

Five previously weighed chitosan aerogel beads were placed in Eppendorf tubes with 1 mL of a tricine buffer solution (pH 7.5) containing collagenase at a concentration of 2 units/mL (37 ºC, 20 rpm). At selected times (0, 0.5 and 4 h), 33 µL aliquots of the enzyme solution were extracted and mixed with 966 µL of a FALGPA solution at a concentration of 48 mg/mL. The reaction was monitored by measuring the changes in absorbance by UV/Vis spectrophotometry at a wavelength of 345 nm (8453, Agilent, Santa Clara, CA, USA) every 15 s for 5 min. The collagenase activity was calculated following the manufacturer guidelines and expressed as

units/mL. A collagenase solution without chitosan aerogel particles was used as the negative control and Milli-Q water was used as blank.

2.3.4. Vancomycin entrapment yield assay

Vancomycin entrapment yield was evaluated by immersing eight aerogel beads of known weight and loaded with vancomycin into Falcon tubes containing 5 mL of HCl 0.1 M under magnetic stirring (750 rpm). After 90 min in the acidic medium, the chitosan particles were completely dissolved, the solutions were centrifuged and the vancomycin concentration in the supernatant was measured by UV/Vis spectrophotometry (8453, Agilent, Santa Clara, CA, USA) at a wavelength of 281 nm. The vancomycin loading and entrapment yield (in percentage) were calculated using Eq. (3) and (4), respectively:

$$\text{Loading (\%)} = \frac{w_P}{w_{aer}} \times 100 \quad (3)$$

$$\text{Entrapment yield (\%)} = \frac{w_P}{w_T} \times 100 \quad (4)$$

where w_P is the amount (mg) of vancomycin hydrochloride measured by the UV/Vis analysis, w_{aer} is the total amount of aerogel (mg), and w_T is the initial amount (mg) of vancomycin added for the preparation of the aerogels. The test was carried out in triplicate. Prior to the measurements, a calibration curve of vancomycin in HCl 0.1 M was obtained and validated in the 25-200 mg/mL range ($R^2 > 0.999$). Chitosan aerogel particles without vancomycin (i.e. blank) were also evaluated to eliminate the interference of chitosan in the UV/Vis measurements.

2.3.5. Vancomycin release from the aerogel particles

Twenty vancomycin-loaded chitosan aerogel particles were weighed, immersed into recipients containing 10 mL of PBS pH 7.4 medium and put into an oscillating bath (P Selecta Unitronic 320 OR, Barcelona, Spain) at 37 ºC and 60 rpm. 2 mL-aliquots of the medium were sampled at selected times (0, 0.25, 0.5, 1, 2, 4, 8, 24, and 48 h) and measured by UV/Vis spectroscopy (8453, Agilent, Santa Clara, CA, USA) at the wavelength of 281 nm. The extracted volume was immediately replaced with equal volumes of fresh PBS medium. Prior to the measurements, a

calibration curve of vancomycin in PBS was obtained and validated in the 5-25 μg/mL range (R^2 > 0.998). The kinetics of the dissolution process of vancomycin hydrochloride powder in PBS pH 7.4 medium was also studied to compare the dissolution profiles of the free and the entrapped drug.

The vancomycin release profile was fitted to a first-order release model according to Eq. (5) and corresponding to a first-order dissolution process reaching a plateau (GraphPad Prism v. 6.04, GraphPad Software, La Jolla, CA, USA):

$$D = (D_0 - D_P) \cdot e^{-k \cdot t} + D_P \quad (5)$$

where *D* denotes the unreleased and/or degraded dosage of vancomycin (in percentage) at time *t*; D_0 is the initial vancomycin dosage in the aerogels (in percentage); D_P is the unreleased and/or degraded dosage (in percentage) of vancomycin in the plateau region; and *k* is the release rate coefficient, in h^{-1}.

2.3.6. Antimicrobial ability of the gels

A susceptible strain of *Staphylococcus aureus* (ATCC 25923) was suspended in 10 mL of simulated body fluid (SBF pH 7.4) to a final concentration of 8.0×10^5 CFU/mL. One chitosan aerogel bead of each formulation loaded with vancomycin (CS1-V5, CS1-V10 and CS1-V20) was sterilized by UV radiation during 1 h and put in contact with 200 μL of the bacterial broth. Free bacterial broth was the negative control. Bacterial broth incubated with free vancomycin powder (0.0665, 0.101 and 0.214 μg/μL, equivalent to the vancomycin payload of the CS1-V5, CS1-V10 and CS1-V20 aerogels, respectively) was the positive control. At different incubation times (6, 24 and 48 h), turbidity was measured at a wavelength of 600 nm in four replicates to monitor the planktonic bacteria. For the same time periods, aliquots of the bacterial suspensions were also taken, serially diluted and the planktonic bacteria quantification was measured by spread-plating in plate count agar in four replicates. The colony forming units (CFUs) were quantified and results expressed as decimal logarithm of the number of planktonic bacteria per milliliter of suspension.

2.3.7. Cytotoxicity assay

BALB/3T3 fibroblasts (10,000 cells/well) were cultured in 24 well-plates in DMEM supplemented with 10% FBS, penicillin 100 U/mL and streptomycin 100 μg/mL. The plates were incubated for 24 h at 37 ºC in a humidified atmosphere with 5% CO_2. Then, CS1-V0, CS1-V5, CS1-V10 and CS1-V20 particles were sterilized by UV radiation during 1 h and placed in each well (in triplicate). DMEM medium and medium with unloaded aerogels acted as blanks, and aerogel-free cell culture was the negative control. After 24 and 48 h of culture, 50 μL of WST-1 reagent (Roche, Basel, Switzerland) were added to each well. Plates were incubated for 4 additional hours, shaken thoroughly for 1 min and the absorbance was measured at a wavelength of 440 nm in a plate reader (EnSpire, PerkinElmer, Madrid, Spain).

2.3.8. Statistical analysis

Quantitative data were subjected to an analysis of variance (one-way ANOVA, Tuckey's test) using a level of significance (α) of 0.05. An unpaired, non-parametric Mann-Whitney test was used to analyze the data obtained from the enzymatic assay, to compare the activities of the free enzyme and the enzyme incubated with the aerogels using a level of significance (α) of 0.05. Statistical analysis were made with GraphPad Prism v. 6.04 (GraphPad Software, La Jolla, CA, USA).

3. Results and discussion

3.1. Morphological and textural properties of the chitosan aerogels

Chitosan hydrogel beads were formed by dripping droplets of a chitosan solution into a basic NaOH 0.1 M solution. In this sol-gel method, the formation of the chitosan gels took place immediately after contact with the gelation bath. The chitosan hydrogels were initially transparent and turned white after *ca.* 1 min in the ageing medium (see Video S-1). The gel beads were spherical and the presence of a tail was noticed depending on the distance of the syringe to the gelation bath (Fig. S-2). After 1 h of ageing, the subsequent solvent exchange to EtOH caused slight volume shrinkage of 11.9 ± 6.3 %. The solvent exchange to ethanol is a usual practice for aerogel processing to facilitate the extraction of the solvent by $scCO_2$ during the drying process. The extraction of water is even more crucial for the case of chitosan

aerogels, since any remnant of water would form carbonic acid in the presence of $scCO_2$ that would cause the partial dissolution of the chitosan gel (Kayser et al., 2012). After the supercritical drying (i.e. alcogel-to-aerogel step), the particles preserved their white and spherical structure, with an overall volume shrinkage of 57.0 ± 4.5 % with respect to the original hydrogels, a similar value to those reported in the literature (Kayser et al., 2012; Quignard et al., 2008). This shrinkage was attributed to the flexibility of the polymeric chains of chitosan that are brought closer after the extraction of the solvent (Quignard et al., 2008). Shrinkage values were much lower than those obtained by freeze-drying and oven drying of the same chitosan hydrogels (95.9 and 97.7%, respectively). Overall porosity of the chitosan aerogel beads was 96.8 ± 0.4 % (CS1-V0 in Table 1), a very high value notably if compared to the traditional evaporative drying and freeze-drying methods (xerogels and cryogels in Table 1, respectively), which are not able to preserve the intrinsic nanoporous structure of the gels.

The highly porous structure of the CS1-V0 chitosan aerogel beads was confirmed by SEM microscopy (Fig. 1). Beads were formed by a network of intermingled polysaccharide fiber bundles. Voids within and between the fiber bundles are mesopores (2-50 nm) and macropores (>50 nm), respectively, according to the IUPAC classification. This dual porous structure of the aerogels was observed in the inner and outer structure of the particles (Fig. 1). Chitosan crystallinity was reduced after the aerogel processing according to the XRD results (Fig. S-3).

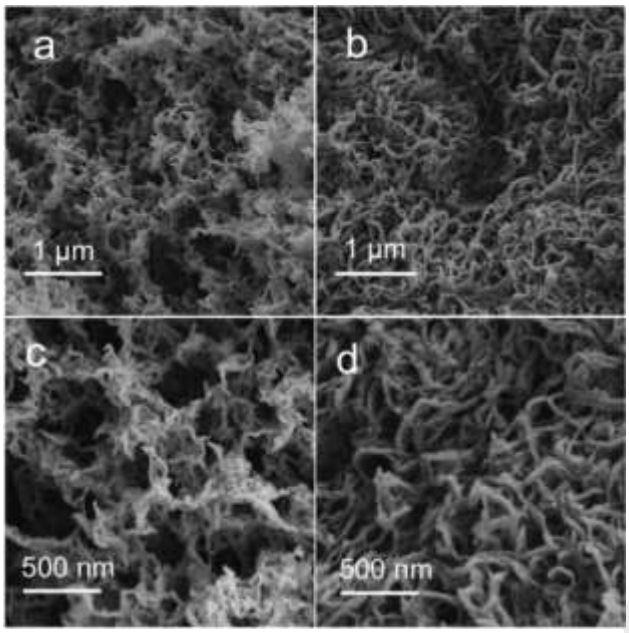

Figure 1. Textural appearance of the (a, c) interior and (b,d) surface of the CS1-V0 chitosan aerogel beads by SEM imaging (x50,000 and x100,000). A dual macroporous and mesoporous distribution was observed for the chitosan aerogels.

The effect of the ageing time of the chitosan hydrogels in the gelation bath on the particle size and porosity of the resulting chitosan aerogels was studied (Table 1). The overall volume shrinkage decreased with ageing time and subsequently larger particles were obtained. Ageing time had a moderate effect on the overall porosity of the aerogels.

Table 1. Influence of the ageing time (0.5, 1, 2, 4, 10 and 24 h) of the chitosan gel beads on the physicochemical properties of the resulting chitosan aerogel particles. Results were statistically compared (ANOVA Tuckey's test, $\alpha < 0.05$). Equal letter denotes statistically homogeneous groups. Notation: ρ_{env}, envelope density; ε, overall porosity.

Particles	**Diameter (mm)**	**ρ_{env} (g/cm^3)**	**ε^1 (%)**	**Overall volume shrinkage (%)**
CS0.5-V0	3.95 (0.12)^{a}	0.046 (0.004)^{a}	96.8 (0.4)^{a}	55.8 (4.0)^{a}
CS1-V0	4.02 (0.12)^{a,b}	0.046 (0.004)^{a}	96.8 (0.4)^{a}	53.3 (4.1)^{a}
CS2-V0	4.05 (0.11)^{b}	0.049 (0.004)^{a}	96.6 (0.4)^{a}	52.6 (3.7)^{a}
CS4-V0	4.35 (0.11)^{c}	0.041 (0.003)^{a}	97.2 (0.3)^{a}	41.3 (4.5)^{b}
CS10-V0	4.42 (0.11)^{c,d}	0.041 (0.003)^{a}	97.2 (0.3)^{a}	38.3 (4.6)^{b}
CS24-V0	4.49 (0.21)^{d}	0.042 (0.006)^{a}	97.1 (0.5)^{a}	35.0 (9.4)^{c}
cryogels	1.68 (0.07)^{e}	0.535 (0.046)^{b}	63.0 (4.4)^{b}	95.9 (0.4)^{d}
xerogels	1.48 (0.06)^{f}	0.900 (0.104)^{c}	37.8 (8.8)^{c}	97.7 (0.3)^{d}

[1] ρ_{skel} of the particles was 1.446 ± 0.116 g/cm^3; values obtained applying Eq. (1); standard deviation was calculated using measurements of *ca.* 50 aerogel beads.

The textural properties (a_{BET}, $V_{P,BJH}$ and $D_{P,BJH}$) of the chitosan aerogel particles gelified at different ageing times were compared by nitrogen adsorption-desorption analysis (Table 2). The textural characterization of the chitosan cryogels and xerogels could not be measured since their mesoporosities were below the detection limit of the equipment (a_{BET} < 5 m^2/g). All aerogels showed isotherms classified as type IV according to the IUPAC recommendations (Sing, 2009), typical from mesoporous materials and characterized by the presence of a hysteresis loop and a high volume of nitrogen adsorbed (inset in Fig. S-4). The mesoporous size distribution attributed to the pores within the chitosan fiber bundles had a log-normal, unimodal distribution according to the BJH-method (Fig. S-4). This mesoporous structure had a mean pore size between 12 to 15 nm depending on the ageing time and was the main responsible of the high specific surface areas obtained for the chitosan aerogels (Table 2). A certain improvement in the textural properties was observed when increasing the ageing time up to 4 h, notably regarding the surface area. The contribution of the mesopore and macropore volumes to the total pore volume was also studied (V_{mes} and V_{MP} in Table 2, respectively). Results indicate that the macropore volume is highly predominant (above 95% in all cases). This volume is attributed to the widely spaced zones of contact between fibril bundles previously observed by SEM imaging. This dual porosity of chitosan aerogels can be of relevance for their use as carriers of antimicrobial agents for wound treatment just after debridement since mesopores provide large surface areas for high loadings of adsorbed drug, whereas macropores favor the drug diffusion upon contact with the exudate environment resulting in fast release rates and quick antimicrobial responses at the wound site.

Overall, an ageing time of 1 h was chosen as a trade-off solution for ulterior development and testing of chitosan aerogels as vancomycin carriers for wound applications. Although intermediate ageing times (4 h) improved the textural properties of the aerogels (Table 2), the high water solubility of the vancomycin hydrochloride (>100 mg/mL) (Varanda et al., 2006) urged to reduce the ageing time to avoid a dramatic drug loss in the ageing medium.

Table 2. Textural properties evaluated by nitrogen adsorption-desorption tests of the chitosan aerogel particles prepared with different ageing times (0.5, 1, 2, 4, 10 and 24 h). Notation: a_{BET}, specific surface area by the BET method; $V_{P,BJH}$, overall specific pore volume obtained by the BJH-method; V_{mes}, specific mesopore volume; V_{MP}, specific macropore volume; $D_{P,BJH}$, mean pore diameter by the BJH-method.

Particles	a_{BET} **(m²/g)**	$V_{P,BJH}$ **(cm³/g)**	$D_{P,BJH}$ **(nm)**	V_{mes} **(cm³/g)**	V_{MP} **(cm³/g)**
CS0.5-V0	360 (18)	1.42 (0.07)	14.1 (0.7)	1.09 (0.05)	20.14 (2.35)
CS1-V0	343 (17)	1.32 (0.07)	14.0 (0.7)	1.03 (0.05)	19.89 (2.21)
CS2-V0	386 (19)	1.56 (0.08)	14.4 (0.7)	1.19 (0.06)	18.35 (2.02)
CS4-V0	479 (24)	1.70 (0.09)	12.6 (0.6)	1.25 (0.06)	22.30 (2.28)
CS10-V0	257 (13)	1.01 (0.05)	14.2 (0.7)	0.79 (0.04)	22.74 (2.03)
CS24-V0	324 (16)	1.32 (0.07)	15.0 (0.8)	0.99 (0.05)	22.28 (3.71)

3.2. Water sorption tests

Moisture balance is essential for the adequate healing process of an exudative wound (Bajjada, 2017). Wound dressings should be able to maintain an optimum moist environment needed for the regeneration process while removing the excess of exudate from the wound, which in turn prevents infection. In this work, the aerogels experienced a weight increase between 300 and 400 % after 30 min in contact with PBS pH 7 (Fig. 2). These water absorption values remained stable at least during the following 24 hours and are comparable or even higher than other bio-based formulations intended for the same application (Gilotra, Chouhan, Bhardwaj, Nandi, & Mandal, 2018).

The pH in the surroundings of the wound varies as a function of the severity (normal or chronic) and the healing stage (Gethin, 2007; Percival, McCarty, Hunt, & Woods, 2014) and influences the associated healing processes. In general, the pH in the wound vicinity moves from basic conditions towards the neutral-to-acidic region as soon as the healing process progresses. Accordingly, the pH values in the chronic wound site are in the 7.2-8.9 range, the epithelialized wound has a pH of 6 and intact skin has a pH of *ca.* 5.5. The water sorption range of the chitosan aerogels was similar in the pH 6-8 range (Fig. 2), so no differences would be expected in the wound site regardless of the usual exudate pH range values.

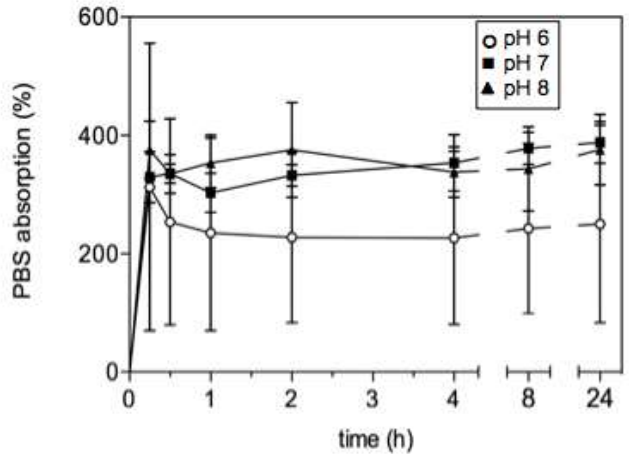

Figure 2. Water absorption as a function of time of CS1-V0 aerogels in contact with PBS medium at different pH values (6, 7 and 8).

3.3. Collagenase activity test

Collagenase is a metalloproteinase that naturally participates in collagen remodeling after an injury, thus favoring the repair of the tissue (Trengove et al., 1999). However, persistent inflammation in some chronic wounds results in the overexpression of metalloproteinases that degrade collagen, a component playing a key role in the proliferative phase of wound healing, not only in the damaged tissue but also in healthy skin tissue.

Results of the collagenase activity in the presence and absence of CS1-V0 chitosan aerogel particles are shown in Table 3. Enzymatic activity results suggested that the presence of chitosan aerogel particles does not inhibit the collagenase activity after 4 hours contact and for the enzymatic concentration tested (2 units/mL). A slight increase in the collagenase activity seems to take place, although not statistically significant. Therefore, a high enzyme adsorption to the aerogel or a non-specific chitosan degradation are not expected, since no activity loss has been observed during the collagenase tests.

Table 3. Collagenase activity expressed in percentage with respect to the initial activity of the enzyme solution alone (Enzyme) and in contact with the chitosan aerogel particles (Enzyme + CS1-V0).

Solution	0.5 h (% initial activity)	4 h (% initial activity)
Enzyme	87.6 (15.6)	70.5 (9.4)
Enzyme + CS1-V0	111.6 (3.8)	95.0 (8.0)

3.4. Vancomycin-loaded aerogels processing and properties

The loading of vancomycin hydrochloride in the chitosan aerogels was performed during the gelation process itself since vancomycin is highly water-soluble. The direct solvent exchange of the gels from water to pure ethanol prevents further drug losses with respect to the use of water:ethanol sequential dilutions series, since vancomycin is poorly soluble in ethanol. After supercritical drying, the vancomycin loading in the CS1-V5, CS1-V10 and CS1-V20 aerogels were 8.5 ± 4.0, 12.9 ± 1.0 and 27.3 ± 2.8 μg/mg of particle, respectively. The corresponding entrapment yields were 12.1 ± 1.0, 12.9 ± 1.0 and 13.7 ± 1.4 %, respectively.

The vancomycin-loaded chitosan aerogels were characterized by ATR-FTIR spectroscopy (Fig. 3). CS1-V20 aerogel had the characteristic stretching bands of the chitosan amino groups at 1588 and 1652 cm^{-1} (X. Chang, Chen, & Jiao, 2008). The main bands from vancomycin (-OH, C=O, C=C and phenolic C-O stretchings at 3450, 1654, 1504 and 1230 cm^{-1}, respectively) (Yao et al., 2013) cannot be observed in the IR spectrum of the aerogel due to the overlapping with bands from chitosan. Nevertheless, the presence of vancomycin in the aerogel can be ascertained by a shoulder at 703 cm^{-1} and a weak band at *ca*. 1600 cm^{-1}, corresponding to the free amino groups and to the amide group from the acetylated amino groups of the drug, respectively (Zarif, Afidah, Abdullah, & Shariza, 2012).

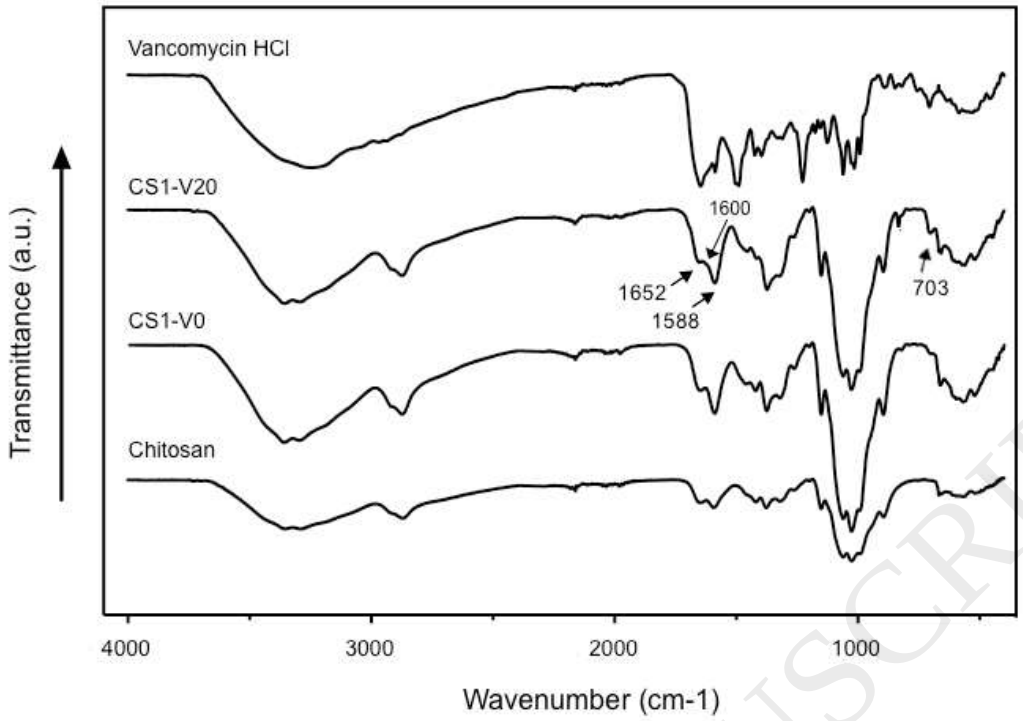

Figure 3. ATR-IR spectra of (a) chitosan powder, (b) CS1-V0 particles, (c) CS1-V20 particles and (d) vancomycin powder.

3.5. Vancomycin release from chitosan aerogels

The vancomycin release from the chitosan aerogel particles followed a first-order release kinetics (Fig. 4). A fast release of vancomycin during the first hour was followed by a slower vancomycin release during the next hours when the unreleased vancomycin content was dramatically reduced. The release was prolonged up to 24 h when the release of vancomycin seemed to reach a plateau. Overall, the aerogel carrier allowed a modified vancomycin release since the complete dissolution of pure vancomycin in PBS medium was faster (with 90% dissolved after 5 min).

The release tests showed that 100% vancomycin release was not observed even at prolonged times (7 days) (Fig. 4). The presence of two different drug fractions 1) drug deposited on the aerogel structure but weakly bound, and 2) drug with a certain drug-chitosan chemical interactions, might explain this release profile. Upon aerogel processing, the step of chitosan gel ageing in the aqueous medium led to significant vancomycin leaching. Anti-solvent precipitation on the gel surface of the vancomycin present in the pore solution can take place

during the ulterior solvent exchange to ethanol (Gurikov & Smirnova, 2018), due to the very low solubility of the drug in ethanol. After supercritical drying, these drug deposits are the source of the vancomycin fraction with fast dissolution in the release medium during the first hours. The second fraction of vancomycin was related to drug molecules with a certain interaction with the chitosan backbone through hydrogen bonding that, after pore water filling and swelling of the gel network, had a very slow release rates limited by the diffusion through the gel as already observed for other vancomycin-polysaccharide gels (Zhao et al., 2014). This vancomycin fraction, obtained by difference between the vancomycin amount loaded and the vancomycin amount released after 8 hours, represented *ca.* 4-6 µg drug/mg of particle and was similar for the three vancomycin-loaded aerogel formulations tested.

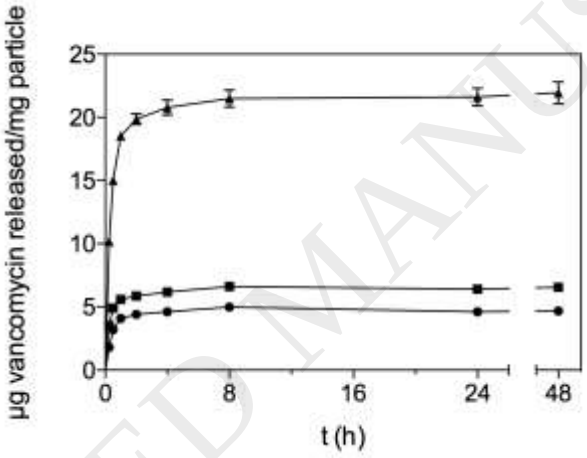

Fig. 4. Vancomycin release profile from chitosan aerogels in PBS pH 7.4 medium (37°C, 60 rpm) during 2 days. Legend: CS1-V5 (circles), CS1-V10 (squares), and CS1-V20 (triangles).

The vancomycin release profile fitted to a first-order release model regardless of the initial vancomycin content used in the aerogel processing (Table 4). The remaining vancomycin dosage (in percentage) in the plateau stage (D_p) was lower for the CS1-V20 aerogels and was related to the processing of this formulation with higher vancomycin contents in the initial hydrogel that favored a higher deposition of weakly bound vancomycin on the gel surface by anti-solvent precipitation.

The release rate coefficients (k) were similar for the three aerogel formulations. According to the wellness of the fitting to this model, the vancomycin mass transfer mechanism from the

aerogel was mainly governed by a combined dissolution and diffusion process. This vancomycin release behavior is considered as representative for the pH range of skin wounds (5.5-8.9) since sink conditions for the drug release are preserved in this range (Faustino, 2008), the slow degradation rate of the aerogel matrix has no influence in the 48-hour timeframe and the matrix swelling is similar for these pH values (Section 3.2).

Wound debridement removes or interrupts the formation of biofilms in chronic wounds. 24-48 h after this clinical practice, there is a suitable timeframe to act against bacterial colonization at the wound site (Albaugh et al., 2013). The local administration of vancomycin with the herein presented aerogel formulation can provide a quick therapeutic response since, after 2 h of contact of the aerogels with the release medium, the vancomycin concentrations in the PBS medium was above the Minimum Inhibitory Concentration (MIC) for *S. aureus* (1-2 μg/mL) (Martinez et al., 2009), the prevailing virulent bacteria in chronic wound infections. Thereafter, the observed release of the antibiotic during the following hours can be effective in maintaining the vancomycin content above the MIC-values to kill the bacterial strains and to prevent the wound site from bacterial recolonization. Thus, the release behaviour of vancomycin in aerogels is expected to maintain local therapeutic levels of vancomycin at the wound site in an *in vivo* environment more effectively than the intrawound application of vancomycin powder (Zebala et al., 2014) by counteracting the local drug losses due to absorption and transport through biological fluids. This release profile is also compatible with the incorporation of these aerogels in wound dressings with exchange frequencies of 24-48 hours.

Table 4. Kinetic fitting parameters of the vancomycin release profiles from drug-loaded chitosan aerogels in PBS solution (pH 7.4) according to Eq. (5). Doses D_0 and D_p are expressed as percentage of unreleased and/or degraded vancomycin. Values are denoted as mean ± standard error

Aerogel	D_0, dose remaining %	D_p, dose remaining %	k, h^{-1}	R^2
CS1-V5	100.2±1.2	43.2±0.5	2.06±0.10	0.988
CS1-V10	99.2±1.7	49.8±0.7	2.78±0.24	0.964
CS1-V20	98.9±1.8	21.3±0.7	2.31±0.13	0.983

3.6. Antimicrobial test

The antimicrobial performance of the vancomycin-loaded aerogels was tested against *S. aureus* bacterial strain incubated in SBF medium. Tests were performed so that the release of vancomycin from the chitosan aerogels provided concentrations in the medium above the Minimum Inhibitory Concentration (MIC) for *S. aureus*.

Antimicrobial evaluation test by CFUs counting showed a time-dependent survival rate of *S. aureus* when in contact with the vancomycin-loaded aerogels (Fig. 5a). The planktonic bacterial concentration increased during the first 6 hours under all the tested incubation conditions, and then only decreased with time in the case of the presence of vancomycin in the formulation (CS1-V5, CS1-V10 and CS1-V20). Accordingly, there were no cultivable planktonic bacteria in the medium after 48 h of incubation in the case of presence of vancomycin-loaded aerogels. The results obtained from the turbidity measurements were consistent with the observed inhibition of bacterial growth (Fig. 5b). Therefore, the bacterial strain was completely inactivated after 48 hours of incubation, for the case of the vancomycin-containing chitosan aerogels. As expected, the bacterial growth was inhibited with the free vancomycin powder just after 6 h of incubation, since all the tested drug concentrations (0.0665, 0.101 and 0.214 µg/µL) were above the MIC for *S. aureus* (Fig. 5b).

Antimicrobial tests showed no bactericidal effect of chitosan by itself, since the results from the negative control (free bacterial growth) and the chitosan aerogels (CS1-V0) were similar. The antimicrobial mechanism of chitosan is the solubilization of the chitosan in the medium and the presence of more $–NH_3^+$ residues in the chitosan molecular structure favors the binding of the polysaccharide to the cell surface causing structural destabilization (Younes et al., 2014). In general, the antimicrobial effect of chitosan is promoted at low molecular weights, high deacetylation degrees (DD>70%) and, mainly, low pHs (pH<6.5). Null or low bactericidal effect of a similar chitosan to the one used in this work have been previously reported at pHs above 7 because of the high proportion of uncharged amino groups in the macromolecule and the poor solubility of chitosan at this pH (Chang et al., 2015; Younes et al., 2014).

In the present work, the chitosan was used as a delivery vehicle for antimicrobial drugs to improve wound healing and treatment, due to its inherent characteristics such as biodegradability, biocompatibility and non-toxicity (Dai, Tanaka, Huang, & Hamblin, 2011; Talebian & Mansourian, 2017). The antimicrobial profiles observed for vancomycin-loaded chitosan aerogels and for the free-form drug emphasize the role of chitosan aerogels as carriers for controlled vancomycin release in an antibacterial treatment. The vancomycin-loaded chitosan aerogel beads showed excellent bactericidal characteristics, killing 98, 99 and 100 % of planktonic bacteria population at 6, 24 and 48 h, respectively, independently of the vancomycin concentration used. The results showed that the vancomycin loading in chitosan aerogels did not affect vancomycin bioactivity and therefore these systems could be a good alternative to prevent the wound site from bacterial colonization.

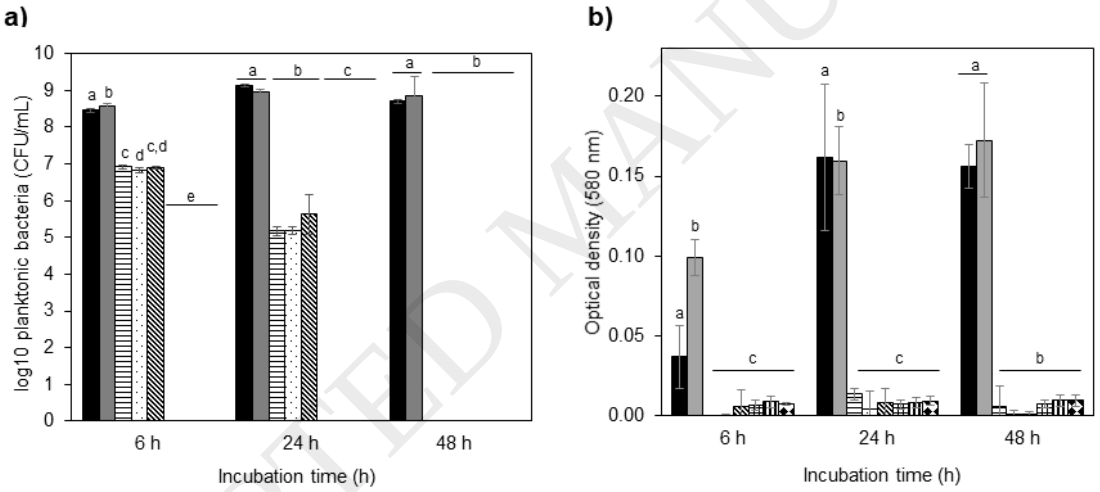

Fig. 5. Quantification by (a) CFUs counting and (b) turbidity measurements of planktonic *S. aureus* bacteria in contact with vancomycin-loaded chitosan aerogel beads or with free vancomycin in SBF pH 7.4 during different incubation times. Legend: without aerogel and vancomycin (black bars), CS1-V0 (grey), CS1-V5 (horizontal bars), CS1-V10 (dots) and CS1-V20 (diagonal bars) aerogels, and free vancomycin at concentrations of 0.665 (grid pattern), 0.101 (vertical bars) and 0.214 μg/μL (diamonds). Results were statistically compared (ANOVA Tuckey's test, $\alpha < 0.05$). Equal letter denotes statistically homogeneous groups. After

48 h, no CFUs were quantified for vancomycin-loaded aerogels. The antimicrobial effect after 24 and 48 h was similar for all the vancomycin concentrations.

3.7. Cytotoxicity assay

Cell viability in the presence of chitosan aerogels were tested using a fibroblast cell line. After 24 h of incubation, all of the aerogel formulations presented a good cytocompatibility with values of cell viability above 80%, and there were no significant differences between the cells in contact with the aerogels and the control group (Fig. 6). After 48 h, the aerogels also presented good cytocompatibility, but the cell viability in the wells cultured with the CS1-V20 aerogels significantly decreased compared to the control group. Several studies have demonstrated that, at high concentrations or after continuous exposure, the vancomycin can present a cytotoxic effect on human cells like fibroblasts (Damour et al., 1992; J. X. Liu et al., 2018). Nevertheless, the cell viability was still acceptable (72.6 ± 4.0%) after 48 h of incubation of cells in contact with CS1-V20 particles.

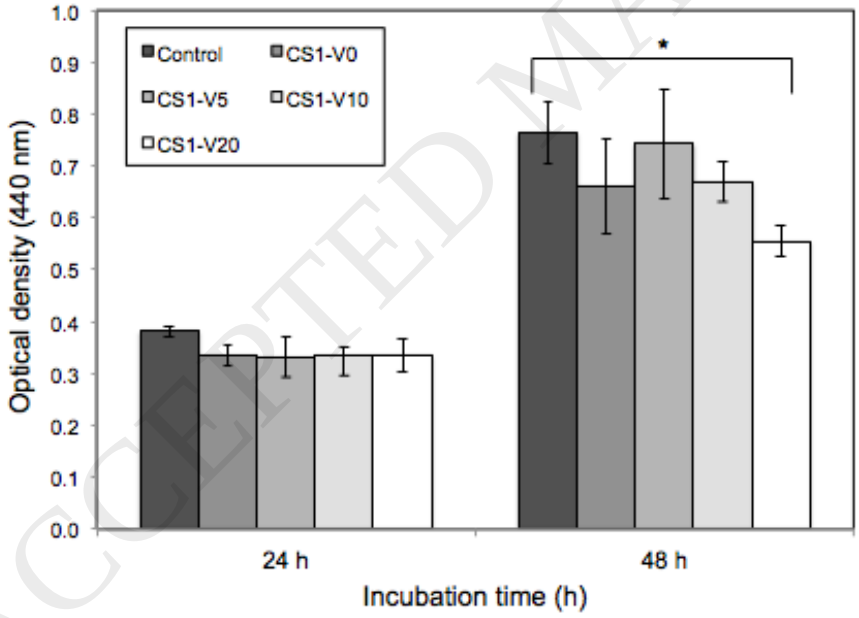

Fig. 6. Optical density measurements of control group of cells and cells cultured with aerogel particles. Asterisk denotes statistical difference between groups ($\alpha < 0.05$) after Tuckey's analysis of variance. A slight cytotoxic effect was noticed in case of the CS1-V20 particles after 48 h of incubation.

4. Conclusions

Chitosan aerogels loaded with a bioactive compound (vancomycin) were herein evaluated regarding their potential use in the management of chronic wounds for the first time. The chitosan aerogel beads had a fibrous structure characterized by a high porosity (> 96%) and large surface area (> 200 m^2/g). Aerogel particles absorbed large amounts of aqueous fluids in the usual exudate pH range (6-8) upon healing, so they would provide an adequate moisture balance in the wound site. Chitosan aerogels did not have any effect on the collagenase activity and therefore they are not expected to interfere with the normal biological healing process. The loading of vancomycin in the aerogels can provide a fast local administration of the antibiotic at the wound site to prevent infections shortly after wound debridement without compromising cell viability. Overall, vancomycin-loaded chitosan aerogels arise as a promising formulation to be incorporated in dressings for the management of chronic wounds, particularly when infectious episodes are expected to take place. Future work will be devoted to adapt the aerogel formulation to a powdered form that could be easily applied to the wound or even incorporated into a multi-layered system and then tested in an *in vivo* animal model of chronic wounds.

5. Acknowledgements

This work was supported by Xunta de Galicia [ED431F 2016/010] & [ED431C 2016/008]; MINECO [SAF2017-83118-R], Agencia Estatal de Investigación (AEI) of Spain and FEDER. C.A. García-González acknowledges to MINECO for a Ramón y Cajal Fellowship [RYC2014-15239].

6. References

Ahmed, S., & Ikram, S. (2016). Chitosan Based Scaffolds and Their Applications in Wound Healing. *Achievements in the Life Sciences, 10*(1), 27–37.

Ahsan, S. M., Thomas, M., Reddy, K. K., Sooraparaju, S. G., Asthana, A., & Bhatnagar, I. (2017). Chitosan as biomaterial in drug delivery and tissue engineering. *International Journal of Biological Macromolecules, 110*, 97-109.

Albaugh, K. W., Biely, S. A., & Cavorsi, J. P. (2013). The Effect of a Cellulose Dressing and Topical Vancomycin on Methicillin-resistant Staphylococcus aureus (MRSA) and Gram-

positive Organisms in Chronic Wounds: A Case Series. *Ostomy Wound Management*, *59*(5), 34–43.

Bajjada, T. (2017). Using a step-up, step-down approach to exudate management. *Journal of Community Nursing*, *31*(2), 34–38.

Bakhsheshian, J., Dahdaleh, N. S., Lam, S. K., Savage, J. W., & Smith, Z. A. (2015). The Use of Vancomycin Powder In Modern Spine Surgery: Systematic Review and Meta-Analysis of the Clinical Evidence. *World Neurosurgery*, *83*(5), 816–823.

Buzia, O. D., Dima, C., & Dima, Ștefan. (2015). Preparation and characterization of chitosan microspheres for vancomycin delivery. *Farmacia*, *63*, 897–902.

Cerchiara, T., Abruzzo, A., Ñahui Palomino, R. A., Vitali, B., De Rose, R., Chidichimo, G., … Luppi, B. (2017). Spanish Broom (Spartium junceum L.) fibers impregnated with vancomycin-loaded chitosan nanoparticles as new antibacterial wound dressing: Preparation, characterization and antibacterial activity. *European Journal of Pharmaceutical Sciences*, *99*, 105–112.

Chang, S.-H., Lin, H.-T. V., Wu, G.-J., & Tsai, G. J. (2015). pH Effects on solubility, zeta potential, and correlation between antibacterial activity and molecular weight of chitosan. *Carbohydrate Polymers*, *134*, 74–81.

Chang, X., Chen, D., & Jiao, X. (2008). Chitosan-Based Aerogels with High Adsorption Performance. *The Journal of Physical Chemistry B*, *112*(26), 7721–7725.

Dai, T., Tanaka, M., Huang, Y.-Y., & Hamblin, M. R. (2011). Chitosan preparations for wounds and burns: antimicrobial and wound-healing effects. *Expert Review of Anti-Infective Therapy*, *9*(7), 857–879.

Damour, O., Zhi Hua, S., Lasne, F., Villain, M., Rousselle, P., & Collombel, C. (1992). Cytotoxicity evaluation of antiseptics and antibiotics on cultured human fibroblasts and keratinocytes. *Burns*, *18*(6), 479–485.

Dhivya, S., Padma, V. V., & Santhini, E. (2015). Wound dressings – a review. *BioMedicine*, *5*(4), 22.

Driscoll, P. (2016, January 21). Global wound care market — double-digit growth from within. Retrieved October 16, 2017, from http://blog.mediligence.com/2016/01/21/global-wound-care-

market-double-digit-growth-from-within/

Faustino, P. J. (2008). *Vancomycin solubility study*. Food and Drug Administration.

García-González, C. A., Alnaief, M., & Smirnova, I. (2011). Polysaccharide-based aerogels—Promising biodegradable carriers for drug delivery systems. *Carbohydrate Polymers*, *86*(4), 1425–1438.

García-González, C. A., Barros, J., Rey-Rico, A., Redondo, P., Gómez-Amoza, J. L., Concheiro, A., Alvarez-Lorenzo, C. & Monteiro, F. J. (2018). Antimicrobial Properties and Osteogenicity of Vancomycin-Loaded Synthetic Scaffolds Obtained by Supercritical Foaming. *ACS Applied Materials & Interfaces*, *10*(4), 3349–3360.

García-González, C. A., Camino-Rey, M. C., Alnaief, M., Zetzl, C., & Smirnova, I. (2012). Supercritical drying of aerogels using CO2: Effect of extraction time on the end material textural properties. *The Journal of Supercritical Fluids*, *66*, 297–306.

García-González, C. A., & Smirnova, I. (2013). Use of supercritical fluid technology for the production of tailor-made aerogel particles for delivery systems. *The Journal of Supercritical Fluids*, *79*, 152–158.

Gethin, G. (2007). The significance of surface pH in chronic wounds. *Wounds UK*, *3*(3), 52-56.

Gilotra, S., Chouhan, D., Bhardwaj, N., Nandi, S. K., & Mandal, B. B. (2018). Potential of silk sericin based nanofibrous mats for wound dressing applications. *Materials Science and Engineering: C*, *90*, 420–432.

Gosain, A., & DiPietro, L. A. (2004). Aging and Wound Healing. *World Journal of Surgery*, *28*(3), 321–326.

Govindarajan, D., Duraipandy, N., Srivatsan, K. V., Lakra, R., Korapatti, P. S., Jayavel, R., & Kiran, M. S. (2017). Fabrication of Hybrid Collagen Aerogels Reinforced with Wheat Grass Bioactives as Instructive Scaffolds for Collagen Turnover and Angiogenesis for Wound Healing Applications. *ACS Applied Materials & Interfaces*, *9*(20), 16939–16950.

Guo, S., & DiPietro, L. (2010). Factors Affecting Wound Healing. *Journal of Dental Research*, *89*(3), 219–229.

Gurikov, P., & Smirnova, I. (2018). Amorphization of drugs by adsorptive precipitation from

supercritical solutions: A review. *The Journal of Supercritical Fluids*, *132*, 105–125.

Harper, D., Young, A., & McNaught, C.-E. (2014). The physiology of wound healing. *Wound Management*, *32*(9), 445–450.

Hiriart-Ramírez, E., Contreras-García, A., Garcia-Fernandez, M. J., Concheiro, A., Alvarez-Lorenzo, C., & Bucio, E. (2012). Radiation grafting of glycidyl methacrylate onto cotton gauzes for functionalization with cyclodextrins and elution of antimicrobial agents. *Cellulose*, *19*(6), 2165–2177.

Jayakumar, R., Prabaharan, M., Sudheesh Kumar, P. T., Nair, S. V., & Tamura, H. (2011). Biomaterials based on chitin and chitosan in wound dressing applications. *Biotechnology Advances*, *29*(3), 322–337.

Kayser, H., Müller, C. R., García-González, C. A., Smirnova, I., Leitner, W., & Domínguez de María, P. (2012). Dried chitosan-gels as organocatalysts for the production of biomass-derived platform chemicals. *Applied Catalysis A: General*, *445-446*, 180–186.

Kosinski, M. A., & Lipsky, B. A. (2010). Current medical management of diabetic foot infections. *Expert Review of Anti-Infective Therapy*, *8*(11), 1293–1305.

Kumar, M. N. V. R., Muzzarelli, R. A. A., Muzzarelli, C., Sashiwa, H., & Domb, A. J. (2004). Chitosan Chemistry and Pharmaceutical Perspectives. *Chemical Reviews*, *104*(12), 6017–6084.

Li, J., Chen, J., & Kirsner, R. (2007). Pathophysiology of acute wound healing. *Clinics in Dermatology*, *25*(1), 9–18.

Liu, J. X., Bravo, D., Buza, J., Kirsch, T., Kennedy, O., Rokito, A., Zuckerman, J. D. & Virk, M. S. (2018). Topical vancomycin and its effect on survival and migration of osteoblasts, fibroblasts, and myoblasts: An *in vitro* study. *Journal of Orthopaedics*, *15*(1), 53–58.

Liu, K.-S., Lee, C.-H., Wang, Y.-C., & Liu, S.-J. (2015). Sustained release of vancomycin from novel biodegradable nanofiber-loaded vascular prosthetic grafts: in vitro and in vivo study. *International Journal of Nanomedicine*, *10*, 885–891.

Luna-Straffon, M. A., Contreras-García, A., Brackman, G., Coenye, T., Concheiro, A., Alvarez-Lorenzo, C., & Bucio, E. (2014). Wound debridement and antibiofilm properties of gamma-ray DMAEMA-grafted onto cotton gauzes. *Cellulose*, *21*(5), 3767–3779.

Maleki, H., Durães, L., García-González, C. A., del Gaudio, P., Portugal, A., & Mahmoudi, M. (2016). Synthesis and biomedical applications of aerogels: Possibilities and challenges. *Advances in Colloid and Interface Science*, *236*, 1–27.

Martinez, L. R., Han, G., Chacko, M., Mihu, M. R., Jacobson, M., Gialanella, P., Nosanchuk, J. D. & Friedman, J. M. (2009). Antimicrobial and Healing Efficacy of Sustained Release Nitric Oxide Nanoparticles Against *Staphylococcus Aureus* Skin Infection. *Journal of Investigative Dermatology*, *129*(10), 2463–2469.

Morton, L. M., & Phillips, T. J. (2016). Wound healing and treating wounds: Differential diagnosis and evaluation of chronic wounds. *Journal of the American Academy of Dermatology*, *74*(4), 589–605.

Muzzarelli, R. A. A. (2011). Chitosan composites with inorganics, morphogenetic proteins and stem cells, for bone regeneration. *Carbohydrate Polymers*, *83*(4), 1433–1445.

Niekraszewicz, A. (2005). Chitosan Medical Dressings. *FIBRES & TEXTILES in Eastern Europe*, *13*(6), 16–18.

Noel, S., Courtney, H., Bumgardner, J., & Haggard, W. (2010). *Chitosan Sponges to Locally Deliver Amikacin and Vancomycin: A Pilot In Vitro Evaluation* (Vol. 468).

O'Neal, P. B., & Itani, K. M. F. (2016). Antimicrobial Formulation and Delivery in the Prevention of Surgical Site Infection. *Surgical Infections*, *17*(3), 275–285.

Pawar, H. V., Boateng, J. S., Ayensu, I., & Tetteh, J. (2014). Multifunctional Medicated Lyophilised Wafer Dressing for Effective Chronic Wound Healing. *Journal of Pharmaceutical Sciences*, *103*(6), 1720–1733.

Percival, S. L., McCarty, S., Hunt, J. A., & Woods, E. J. (2014). The effects of pH on wound healing, biofilms, and antimicrobial efficacy. *Wound Repair and Regeneration*, *22*(2), 174–186.

Pierre, A. C., & Pajonk, G. M. (2002). Chemistry of Aerogels and Their Applications. *Chemical Reviews*, *102*(11), 4243–4266.

Quignard, F., Valentin, R., & Di Renzo, F. (2008). Aerogel materials from marine polysaccharides. *New Journal of Chemistry*, *32*(8), 1300–1310.

Rinki, K., Dutta, P. K., Hunt, A. J., Macquarrie, D. J., & Clark, J. H. (2011). Chitosan Aerogels

Exhibiting High Surface Area for Biomedical Application: Preparation, Characterization, and Antibacterial Study. *International Journal of Polymeric Materials and Polymeric Biomaterials*, *60*(12), 988–999.

Şahin, İ., Özbakır, Y., İnönü, Z., Ulker, Z., & Erkey, C. (2018). Kinetics of Supercritical Drying of Gels. *Gels*, *4*(1).

Sing, K. S. W. (2009). Reporting physisorption data for gas/solid systems with special reference to the determination of surface area and porosity (Recommendations 1984). *Pure and Applied Chemistry*, *57*(4), 603–619.

NHS NEW Devon CCG, *South & West Devon Formulary, Chapter 17. Wound management*, https://southwest.devonformularyguidance.nhs.uk/formulary/chapters (last accessed: 10/09/2018).

Talebian, A., & Mansourian, A. (2017). Release of Vancomycin from electrospun gelatin/chitosan nanofibers. *Materials Today: Proceeding*, *4*, 7065–7069.

Trengove, N. J., Stacey, M. C., Macauley, S., Bennett, N., Gibson, J., Burslem, F., Murphy, G. & Schultz, G. (1999). Analysis of the acute and chronic wound environments: the role of proteases and their inhibitors. *Wound Repair and Regeneration*, *7*(6), 442–452.

Varanda, F., Pratas de Melo, M. J., Caço, A. I., Dohrn, R., Makrydaki, F. A., Voutsas, E., Tassios, D. & Marrucho, I. M. (2006). Solubility of Antibiotics in Different Solvents. 1. Hydrochloride Forms of Tetracycline, Moxifloxacin, and Ciprofloxacin. *Industrial & Engineering Chemistry Research*, *45*(18), 6368–6374.

Wu, T., Zivanovic, S., Draughon, F. A., Conway, W. S., & Sams, C. E. (2005). Physicochemical Properties and Bioactivity of Fungal Chitin and Chitosan. *Journal of Agricultural and Food Chemistry*, *53*(10), 3888–3894.

Xiong, L., Pan, Q., Jin, G., Xu, Y., & Hirche, C. (2014). Topical intrawound application of vancomycin powder in addition to intravenous administration of antibiotics: A meta-analysis on the deep infection after spinal surgeries. *Orthopaedics & Traumatology: Surgery & Research*, *100*(7), 785–789.

Yao, Q., Nooeaid, P., Roether, J. A., Dong, Y., Zhang, Q., & Boccaccini, A. R. (2013).

Bioglass®-based scaffolds incorporating polycaprolactone and chitosan coatings for controlled vancomycin delivery. *Ceramics International*, *39*(7), 7517–7522.

Younes, I., Sellimi, S., Rinaudo, M., Jellouli, K., & Nasri, M. (2014). Influence of acetylation degree and molecular weight of homogeneous chitosans on antibacterial and antifungal activities. *International Journal of Food Microbiology*, *185*, 57–63.

Zarif, M. S., Afidah, A., Abdullah, J. M., & Shariza, A. (2012). Physicochemical characterization of vancomycin and its complexes with β-cyclodextrin. *Biomedical Research*, *23*, 513–520.

Zebala, L. P., Chuntarapas, T., Kelly, M. P., Talcott, M., Greco, S. & Riew, K. D. (2014) Intrawound Vancomycin Powder Eradicates Surgical Wound Contamination. An in Vivo Rabbit Study. *The Journal of Bone and Joint Surgery*, *96*, 46-51.

Zhao, Y., Zhang, X., Wang, Y., Wu, Z., An, J., Lu, Z., Mei, L. & Li, C. (2014). In situ cross-linked polysaccharide hydrogel as extracellular matrix mimics for antibiotics delivery. *Carbohydrate Polymers*, *105*(Supplement C), 63–69.